Progress In Electromagnetics Research, Vol. 135, 331–346, 2013

COMPARISON OF DIFFERENT METHODS FOR THE EXPERIMENTAL ANTENNA PHASE CENTER DETERMINATION USING A PLANAR ACQUISITION SYSTEM

Pablo Padilla[1, *], Jose M. Fernández[2], Jose L. Padilla[1], Gonzalo Expósito-Domínguez[2], Manuel Sierra-Castañer[2], and Belen Galocha[2]

[1]Universidad de Granada-CITIC, Granada, Spain

[2]Technical University of Madrid (Universidad Politécnica de Madrid — UPM), Madrid, Spain

Abstract—This work provides the comparison of different methods for the experimental determination of the phase center location of an antenna. The phase center position is determined by means of measured data obtained with a planar scanning system and computed with different methods: a least-squares fit method with and without weighting coefficients and a directivity-based plane wave spectrum (PWS) analysis method. A study of the phase center position for different microwave antennas is provided. The results of the different methods are presented and compared, along with the confidence interval of the phase center values due to the uncertainties of the acquisition system.

1. INTRODUCTION

Nowadays, wireless communication systems have become an issue of great concern. The possible services and applications to be provided by means of these wireless systems are very diverse and demanding [1–4]. Thus, the requirements of the communication systems and terminals are very severe, as it can be easily seen in the literature [5–9]. The severe requirements usually imply the use of higher and higher working frequencies, such as microwave or even millimeter band [10, 11]. One important issue related to the radiating terminals is its proper and accurate characterization [12] and one usual problem is the accurate

Received 21 November 2012, Accepted 17 December 2012, Scheduled 24 December 2012

* Corresponding author: Pablo Padilla (pablopadilla@ugr.es).

determination of the radiation pattern and the phase center of the antenna. This article is focused in this last topic.

The most common procedures to determine the phase center location of a radiating element are derived from spherical measurements. In these methods [13, 14], the phase center is experimentally determined searching the equi-phase sphere around the radiating direction of the antenna. Thus, the center of the surface obtained corresponds to the phase center of the antenna under test [15]. In this case, phase measurements are obtained by rotating the antenna in the test zone, by means of a rotational measuring system. As a drawback, the rotational measurement systems at microwave or mm-wave frequencies suffer from accuracy problems, providing results with high level of uncertainty [16, 17]. This level of uncertainty in the phase measurements is translated directly into an uncertainty interval in the final computed value of the phase center of the antenna. Considering these uncertainties, the rotary joint of the spherical measuring systems is one critical problem: ripples are introduced into the amplitude and the phase values acquired, yielding the uncertainty of the phase pattern. The main purpose in this work is to explore the phase center determination avoiding spherical methods. Thus, in this work, different methods are proposed to compute the phase center position using planar acquisition systems.

In the document below, the main considerations about the planar measurement configuration used along with the different methods proposed for phase center determination are provided. In addition, the phase center determination for different antennas is computed in order to validate and to compare the different methods. Also reference of the confidence interval $(1-\sigma)$ of the phase center location is provided.

The document is organized as follows: In Section 2, different analysis methods for phase center determination are provided, together with their inherent confidence interval. Section 3 provides the experimental results of the phase center position of some microwave antennas, by means of the proposed analysis methods, along with the comparison between them. Eventually, in Section 4, conclusions are drawn.

2. PHASE CENTER DETERMINATION

Different methods for the computation of the phase center using a planar measuring system [18, 19] are considered in this work. These methods are provided below: Subsection 2.1 makes reference to least-squares fit methods, meanwhile Subsection 2.2 makes reference to directivity-based methods. In Subsection 2.3, the uncertainty analysis

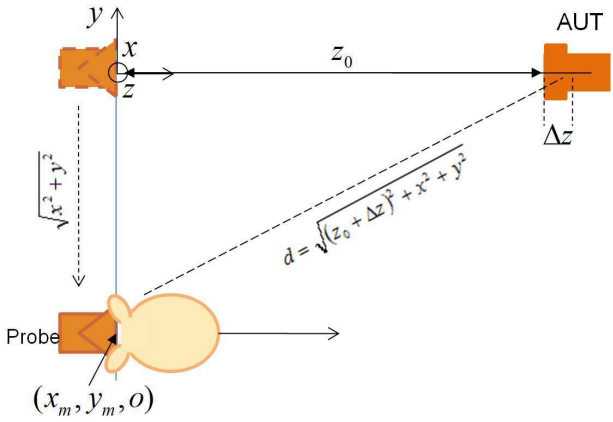

Figure 1. Setup for the least-squares fit method. The tip of the antenna is located at the origin of the coordinate system. The measurement grid is placed in the x-y plane at $z = z_0$.

for these methods is provided.

2.1. Least-squares Fit

The computation of the phase center of an antenna by means of the least-squares fit method implies the comparison between the measured phase value at each point of the planar measuring grid and the theoretical expected one in the grid, for different distances z. For a range of distances, the one that provides the lowest error (difference between theoretical results and measured ones in all the points of the grid) is the one that determines the phase center position. To minimize the deviation between theory and measurements, the least-squares fit procedure is applied with both the theoretical and measured phase values, as given in Fig. 1. Equation (1) yields the calculation of the minimum phase deviation for the least-squares fit, for different distances from the probe. Variables x_n and y_m identify the measurement points in the 2D x-y measuring grid.

$$S(\Delta z) = \min \sum_n \sum_m (\varphi_{meas.}(x_n, y_m, z_0) - \varphi_{th}(x_n, y_m, z_0 + \Delta z))^2 \quad (1)$$

$$\varphi_{th}(x_n, y_m, z_0 + \Delta z) = \frac{2\pi}{\lambda} \sqrt{(z_0 + \Delta z)^2 + x_n^2 + y_m^2} \quad (2)$$

where z_0 is the fixed distance from the outer plane of the antenna under test (AUT), located at the origin, to the measurement grid, z the distance from the tip to the phase center, and $\varphi_{meas}(x_n, y_m, z_0)$ and $\varphi_{th}(x_n, y_m, z_0 + z)$ are the measured and theoretical phase values at each point (x_n, y_m) of the grid, respectively.

A possible variation of the method consists on considering weighting coefficients for the different samples of the summation. This variation is based on the next assumption: the values corresponding to points placed far away from the main radiation direction can be considered less representative in the phase value computation, meanwhile the ones in the main radiation direction are the fundamental ones. The weighting coefficients are identified with the values of the amplitude in the radiation pattern, normalized to the highest amplitude value as shown in (3).

$$S(\Delta z)=\min \sum_n \sum_m A_{nm}(\varphi_{meas}(x_n, y_m, z_0)-\varphi_{th}(x_n, y_m, z_0+\Delta z))^2 \quad (3)$$

where $A_{mn}\,(x_n,\ y_m)$ is the normalized measured amplitude at each point of the grid.

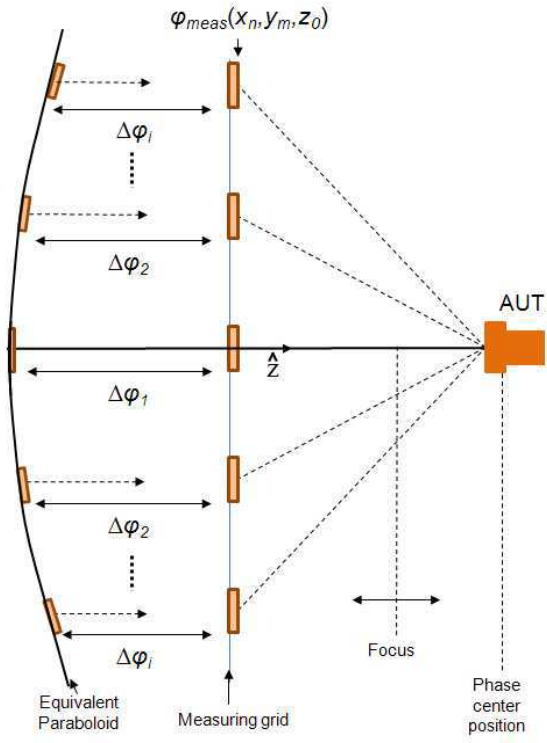

Figure 2. Iterative phase center determination by means of focal length variation of the parabolic reflector to find maximum directivity and the corresponding location of the antenna phase center.

2.2. Directivity-based Analysis Method

The alternative method proposed in this work is derived from the idea of applying the antenna under test as a feeder for a parabolic reflector. The parabolic reflector transforms a spherical wave front to a planar one when the source of the spherical wave front is placed in the focus of the reflector. Thus, it is possible to determine the position of the antenna phase center by computing the directivity over a well-defined parabolic reflector. Then, in the proposed method, the z-coordinate of the antenna regarding the reflector is iteratively varied until its apparent phase center and the focus of the reflector coincide, yielding the global maximum of directivity. A planar wave front emerges only when the focus coincides with the phase center of the antenna. Fig. 2 outlines this scheme.

The above-mentioned iterative procedure for the determination of the highest directivity value can be performed computationally using the measured radiation pattern of the antenna in the planar grid and a conceptual parabolic reflector antenna. However, the proposed analysis method may be simplified, considering that the available data comes from a planar acquisition system. The consideration of the conceptual reflector can be replaced with the calculation of the plane

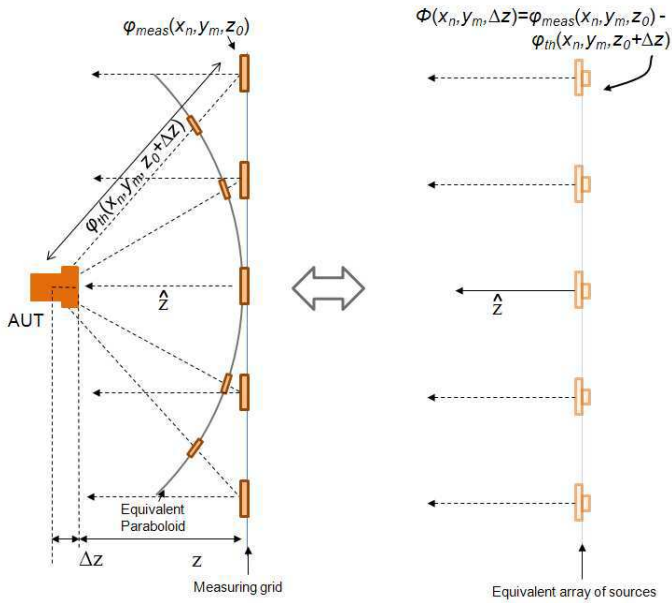

Figure 3. Equivalent array of sources, with the proper choice of phase value in each point of the array.

wave spectrum (PWS) of the equivalent array of sources, with the proper choice of the amplitude and phase value in each point of the array. Fig. 3 depicts the equivalent configuration to be considered.

The conceptual parabolic reflector is replaced by the equivalent array of sources placed at the measurement plane. The PWS of the equivalent array is as follows:

$$F(k_x,k_y,\Delta z)=\sum_m\sum_n A_{meas}\exp(j\phi(x_n,y_m,\Delta z)+jnk_x\Delta x+jmk_y\Delta y) \quad (4)$$

$$\phi(x_n,y_m,\Delta z)=\varphi_{meas}(x_n,y_m,z_{meas})-\varphi_{th}(x_n,y_m,z_{meas}+\Delta z) \quad (5)$$

where, again, $A_{mn}\,(x_n, y_m, z_0)$ and $\varphi_{meas}\,(x_n, y_m, z_0)$ are the measured amplitude and phase at each point (x_n, y_m) of the measuring grid, $d_{x/y}$ is the distance between points in the grid, k_x and k_y are the components of the wave vector in Cartesian coordinate system and m and n are the reference to the location of the different points in the grid. $\varphi_{th}\,(x_n, y_m, z_0 + z)$ is the expected phase value at each point of the grid, according to (2). In this scenario, the phase center of the antenna coincides with the value of $z_0 + z$, which provides the highest directivity $D_{\max}$ estimation from the PWS, according to (6).

$$D(\Delta z)=\frac{F_{\max}}{\iint F(k_x,k_y,\Delta z)dk_xdk_y} \quad (6)$$

2.3. Uncertainty Evaluation

In the experimental determination of the phase center location, the confidence interval is as important as the final result and depends directly on the uncertainty in the outcomes of the measurement system [9]. Considering error propagation, the resulting uncertainty of each method is obtained, for the worst case. In order to obtain the uncertainty of the antenna phase center location, the global uncertainty of the different methods have to be computed, by means of the uncertainty of the electric field value measured at each measuring point of the grid, considering error propagation theory for the computation. The uncertainty of the least-squares fit method without weighting coefficients is given in (7). Meanwhile, the one including these coefficients is included in (8).

$$\delta S=\sum_n\sum_m(2\,|\varphi_{meas}(n,m)-\varphi_{th}|\,\delta\varphi_{meas}) \quad (7)$$

$$\delta S=\sum_n\sum_m(\varphi_{meas}(n,m)-\varphi_{th})^2\delta A + 2\,|A(n,m)(\varphi_{meas}(n,m)-\varphi_{th})|\,\delta\varphi_{meas}) \quad (8)$$

where $\varphi_{meas}(n,m)$ and $A(n,m)$ are the measured values and δ_{meas} and δ_A the associated errors. In the case of (6), its associated error is given in (9).

$$\delta D = \frac{\sum_n \sum_m (A + |A|(\delta\phi))}{\iint_{k_x k_y} (\sum_n \sum_m (\delta A + |A|(\delta\phi + nk_x\delta\Delta x + mk_y\delta\Delta y)))} \quad (9)$$

3. PHASE CENTER DETERMINATION: EXPERIMENTAL RESULTS

In this section, different antennas are measured and the results obtained in the planar acquisition system are processed in order to derive the phase center position with the three methods previously mentioned. Three different microwave antennas are considered and measured at a number of frequencies within their frequency range.

3.1. Antennas under Test

Some details of the antennas considered for the evaluation and comparison of the different methods are provided in Table 1. Images of some of these antennas are shown in Fig. 4.

3.2. Measurement Setup and Measuring Facility

The planar setup for measurements is configured as follows (Fig. 5):

- $A = z_0 = 1.57\,\text{m}$.

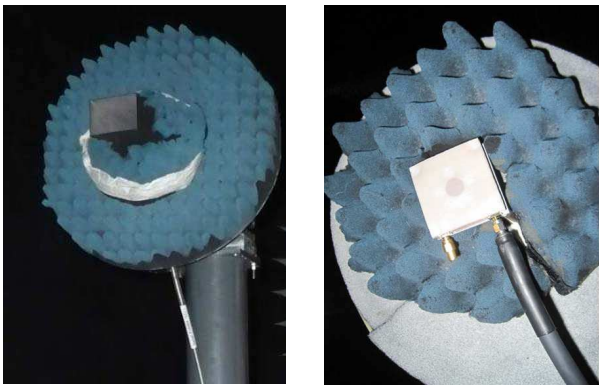

(a) (b)

Figure 4. Antennas under test in the planar system. (a) Rectangular horn (10 GHz to 13 GHz band). (b) Patch antenna at (7.25 GHz to 8.4 GHz band).

Table 1. Details of the antennas under test for the validation and comparison of the different methods for phase center determination.

	Rectangular horn (10 GHz to 13 GHz band)	Rectangular horn (7.25 GHz to 8.4 GHz band)	Patch antenna (7.25 GHz to 8.4 GHz band)
Frequency (GHz)	12	7.75	7.75
Bandwidth (GHz)	3	1.15	1.15
Measured Freq. (GHz)	10, 11, 12, 13	7.25, 7.825, 8.4	7.25, 7.825, 8.4
Distance to probe (m)	1.57	1.57	1.57
Measuring grid (mm)	10	15	15
Polarization	linear	linear	circular

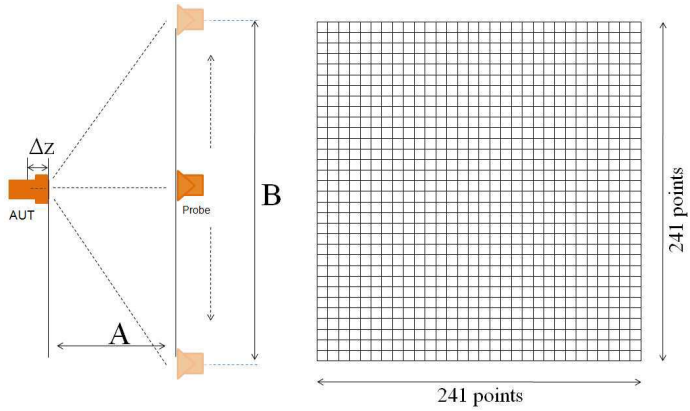

Figure 5. Measurement setup for the planar acquisition: $A = 1.57\,\text{m}$, $B = 1.8\,\text{m}$, rectangular measuring grid of 241 points.

- $B = 1.8\,\text{m}$ both in x- and y-coordinates. This dimension, together with z_0, results in about a $\pm 37°$ field of view.

The pattern is acquired for a rectangular grid ($\Delta x = \Delta y = 10\,\text{mm}$, for the 10 GHz to 13 GHz band, and 15 mm, for the 7.25 GHz to 8.4 GHz

band, respectively).

The planar measurement system used in this work (in Fig. 6) is one of the measuring systems of the antenna measurement facilities of the Technical University of Madrid (UPM). This planar system is a highly accurate system, as it is calibrated for highly demanding measurement requirements. These facilities are a reference measuring laboratory for antenna measurement in Spain and Europe.

3.3. Probe Compensation

The antenna phase and amplitude patterns are corrected by means of the subtraction of the probe pattern, as the effects of the probe have

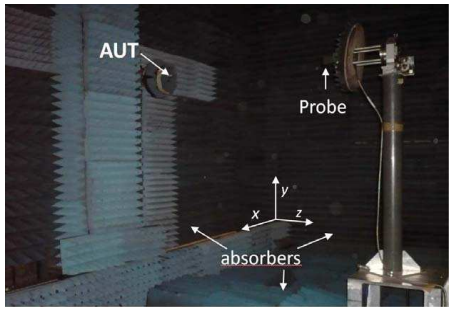

Figure 6. Planar acquisition system in the anechoic chamber.

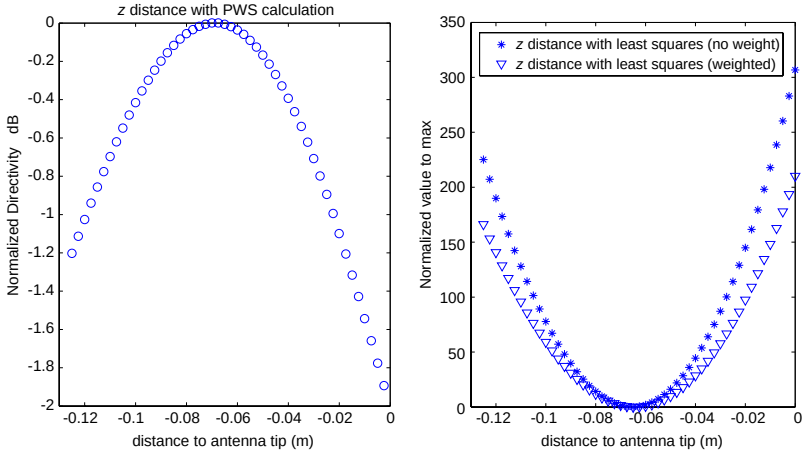

Figure 7. Example of the iterative procedure for the phase center computation, (a) by means of the directivity maximization (PWS method), (b) with the least-square fit procedure.

to be eliminated from the measurements [20, 21]. The probe patterns (amplitude and phase) are acquired using two identical horn probes. The measured patterns contain information of both antennas working together and are corrected accordingly. The horn probes are calibrated horns of the measuring system and their phase center positions are accurately known.

3.4. Phase Center Location Results

The measurements acquired with the planar scanner system, subtracting the probe effect, are processed to derive the phase center position of the three different microwave antennas, with the different approaches previously described. Fig. 7 shows an example of the iterative procedure for the computation of the distance by means of the PWS method (directivity maximization). Figs. 8, 9 and 10 provide the phase center location results for these antennas.

The tolerances of the planar measuring system considered in this work have been widely studied [22–24], according to the literature [25–29], and they are not matter of this work. Information about different

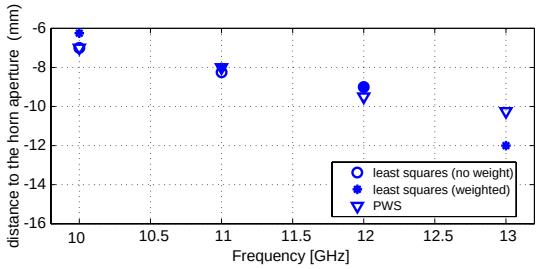

Figure 8. Comparison between phase center positions offered by the different analysis methods within the frequency range, for the 10 GHz to 13 GHz band horn.

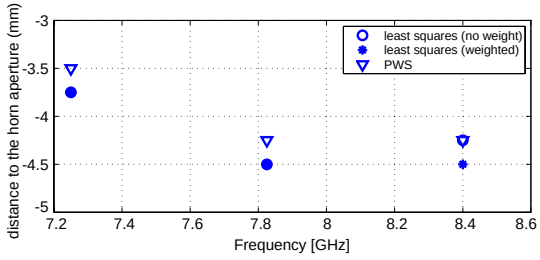

Figure 9. Comparison between phase center positions offered by the different analysis methods within the frequency range, for the 7.25 GHz to 8.4 GHz horn.

Table 2. Uncertainties of the planar measuring system.

Error Sources	**Standard Uncertainty (σ) (dB)**
Stray signals:	
Reflectivity level	0.001
Multiple reflections	0.010
AUT scattering	0.015
Mechanical Set-up inaccuracies:	
Antenna tower pointing, Axes intersection, Probe position, Planarity of the scanner	0.010
Measurement distance	0.001
Electrical System:	
Thermal drift	0.000
Noise	0.000
Receiver non-linearity	0.008
Flexing cables and rotary joints	0.027
Leakage and crosstalk	0.003
Related to Probe:	
Probe Polarization Purity & Probe Pattern	0.005
Truncation errors:	
Truncation errors	0.027
Global Standard Uncertainty	**0.053**
Translated Amplitude and phase error	
Amplitude δA	0.06
Phase $\delta\varphi$	11°

tolerances of the measuring system is provided in Table 2. In this table, the uncertainties of the different parameters and factors in the measuring system are provided: all of them configure the final global uncertainty value of each acquisition, in terms of measured electric field.

According to the measurements and their processing, along with the system tolerances, a comparison among the considered methods, for the three antennas, is provided. Table 3 summarizes the phase center location results along with tolerances.

The above-mentioned results are based on the selection of the $\pm 37^\circ$ field of view. Different choice of the field of view might result in

Table 3. Uncertainties of the planar measuring system.

Rectangular horn (10 GHz to 13 GHz band) (distance to the horn aperture)			
Frequency (GHz)	Least-sq (no weight) (mm)	Least-sq (weighted) (mm)	PWS (mm)
10	-7 ± 1.5	-6.25 ± 2.25	-7 ± 0.75
11	-8.25 ± 1.5	-8 ± 2.5	-8 ± 0.85
12	-9 ± 1.5	-9 ± 2.5	-9.5 ± 0.85
13	-14.25 ± 2.5	-12 ± 3.75	-10.25 ± 1.1
Rectangular horn (7.25 GHz to 8.4 GHz band) (distance to the horn aperture)			
Frequency (GHz)	Least-sq (no weight) (mm)	Least-sq (weighted) (mm)	PWS (mm)
7.25	-3.75 ± 2.5	-3.75 ± 0.85	-3.5 ± 0.8
7.825	-4.5 ± 2.25	-4.5 ± 1.25	-4.25 ± 0.95
8.4	-4.25 ± 2.2	-4.5 ± 1.35	-4.25 ± 1
Patch antenna (7.25 GHz to 8.4 GHz band) (distance to the upper layer of the patch)			
Frequency (GHz)	Least-sq (no weight) (mm)	Least-sq (weighted) (mm)	PWS (mm)
7.25	-4.75 ± 1.65	-4.75 ± 1.15	-4.5 ± 0.8
7.825	-5.5 ± 1.75	-5.75 ± 1.25	-5 ± 0.85
8.40	-4.5 ± 2.5	-4.5 ± 1.75	-4.25 ± 0.95

slightly different phase center position.

The phase center of the probe for each frequency and the distances of the measurement scheme are known and they are taken into account in the results. When the results are analyzed, it is stated that there is a slight difference between the PWS analysis method and the least-squares fit method (either considering weighting coefficients or not). However, it can be noticed that least-squares fit methods are not considering any kind of tendency in the summation error: although the phase difference between theory and measurements can be positive or negative, only the square value is considered in the summation. This is not the case in the PWS method, as the phase error at each point of

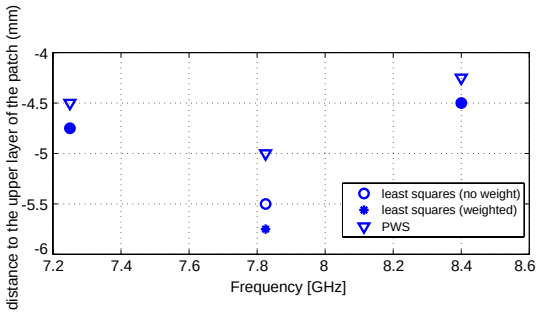

Figure 10. Comparison between phase center positions offered by the different analysis methods within the frequency range, for the patch antenna.

the grid, regarding the theoretical one, computes along with its positive or negative nature. Also a lower value of the error margin is obtained with the PSW method, compared to the least-squares fit methods, as it is provided in Figs. 8 and 9. Furthermore, the proposed PWS analysis can be also applied in the design of reflector-based radiating systems, not only to decide the position of the antenna regarding the focus, but also to extract the possible directivity reduction in the complete system due to a possible small misplacement of the feeding antenna regarding the focus location.

4. CONCLUSIONS

At microwave and mm-wave frequencies, planar scanning systems are a proper alternative to rotation-based measuring systems. In this work, planar scanning is considered and measuring data are analyzed with different analysis methods for the phase center determination: the least-squares fit method with and without weighting coefficients, and the PWS analysis method proposed in this document. This last method, a directivity-based analysis method, provides valuable results as it gives importance to the application of the antenna under test as a feed of a parabolic reflector. Experimental results are obtained at different frequencies for three different microwave antennas. Although the results provided by these three methods are quite similar in terms of the antenna phase center location, the uncertainty of the phase center value and its interval of confidence is much lower in the case of the PWS method. Thus, although the least-squares fit method (either with or without weighting coefficients) is widely used for phase center determination, the PWS method provides better results in terms of accuracy.

REFERENCES

1. Li, X., J. Liao, Y. Yuan, and D. Yu, "Eye-shaped segmented reader antenna for near-field UHF RFID applications," *Progress In Electromagnetics Research*, Vol. 114, 481–493, 2011.
2. Panda, J. R. and R. S. Kshetrimayum, "A printed 2.4 GHz/5.8 GHz dual-band monopole antenna with a protruding stub in the ground plane for WLAN and RFID applications," *Progress In Electromagnetics Research*, Vol. 117, 425–434, 2011.
3. El Maazouzi, L., A. Mediavilla, and P. Colantonio, "A contribution to linearity improvement of a highly efficient Pa for WiMAX applications," *Progress In Electromagnetics Research*, Vol. 119, 59–84, 2011.
4. Exposito-Dominguez, G., J.-M. Fernandez Gonzalez, P. Padilla, and M. Sierra-Castaner, "Dual circular polarized steering antenna for satellite communications in X band," *Progress In Electromagnetics Research*, Vol. 122, 61–76, 2012.
5. Ahdi Rezaeieh, S. and M. Kartal, "A new triple band circularly polarized square slot antenna design with crooked T and F-shape strips for wireless applications," *Progress In Electromagnetics Research*, Vol. 121, 1–18, 2011.
6. Kusuma, A. H., A.-F. Sheta, I. M. Elshafiey, Z. Siddiqui, M. A. S. Alkanhal, S. Aldosari, S. A. Alshebeili, and S. F. Mahmoud, "A new low SAR antenna structure for wireless handset applications," *Progress In Electromagnetics Research*, Vol. 112, 23–40, 2011.
7. Kim, D.-O., N.-I. Jo, H.-A. Jang, and C.-Y. Kim, "Design of the ultrawideband antenna with a quadruple-band rejection characteristics using a combination of the complementary split ring resonators," *Progress In Electromagnetics Research*, Vol. 112, 93–107, 2011.
8. Montero-de-Paz, J., E. Ugarte-Munoz, F. J. Herraiz-Martinez, V. Gonzalez-Posadas, L. E. Garcia-Munoz, and D. Segovia-Vargas, "Multifrequency self-diplexed single patch antennas loaded with split ring resonators," *Progress In Electromagnetics Research*, Vol. 113, 47–66, 2011.
9. Peng, H.-L., W.-Y. Yin, J.-F. Mao, D. Huo, X. Hang, and L. Zhou, "A compact dual-polarized broadband antenna with hybrid beam-forming capabilities," *Progress In Electromagnetics Research*, Vol. 118, 253–271, 2011.
10. Andres-Garcia, B., L. E. Garcia-Munoz, D. Segovia-Vargas, I. Camara-Mayorga, and R. Gusten, "Ultrawideband antenna

excited by a photomixer for terahertz band," *Progress In Electromagnetics Research*, Vol. 114, 1–15, 2011.

11. Xu, O., "Diagonal horn gaussian efficiency enhancement by dielectric loading for submillimeter wave application at 150 GHz," *Progress In Electromagnetics Research*, Vol. 114, 177–194, 2011.
12. Ayestaran, R. G., J. A. Lopez-Fernandez, and F. Las-Heras, "Self-calibration for fault or obstacle correction in continually rotating array antennas," *Progress In Electromagnetics Research*, Vol. 111, 365–380, 2011.
13. Beeckman, P. A., "Analysis of phase errors in antenna-measurements applications to phase-pattern corrections and phase-centre determination," *Microwaves, Antennas and Propagation, IEE Proceedings H*, Vol. 132, No. 6, 391–394, Oct. 1985.
14. Li, P. and L. Jiang, "The far field transformation for the antenna modeling based on spherical electric field measurements," *Progress In Electromagnetics Research*, Vol. 123, 243–261, 2012.
15. Wang, Y. G., J. Wang, Z. Q. Zhao, and J. Y. Yang, "A novel method to calculate the phase center of antennas," *Journal of Electromagnetic Waves and Applications*, Vol. 22, Nos. 2–3, 239–250, 2008.
16. Selvan, K. T., "A modified three-antenna gain measurement method to simplify uncertainty estimation," *Progress In Electromagnetics Research*, Vol. 57, 197–208, 2006.
17. Mallat, J., A. Lehto, and J. Tuovinen, "Antenna phase pattern measurements at millimeter wave frequencies using the differential phase method with only one power meter," *International Journal of Infrared and Millimeter Waves*, Vol. 15, No. 9, 1497–1506, 1994.
18. Padilla, P., P. Pousi, A. Tamminen, J. Mallat, J. Ala-Laurinaho, M. Sierra-Castañer, and A. V. Raisanen, "Experimental determination of DRW antenna phase center at mm-wavelengths using a planar scanner: Comparison of different methods," *IEEE Trans. on Antennas and Propagation*, Vol. 59, No. 8, 2806–2812, Aug. 2011.
19. Padilla, P., P. Pousi, A. Tamminen, J. Mallat, J. Ala-Laurinaho, M. Sierra-Castañer, and A. V. Raisanen, "MM-wave DRW antenna phase centre determination," *2010 Proceedings of the Fourth European Conference on Antennas and Propagation (EuCAP)*, 1–4, Apr. 12–16, 2010.
20. Wang, J., "An examination of the theory and practices of planar near-field measurements," *IEEE Trans. on Antennas and Propagation*, Vol. 36, No. 6, 746–753, Jan. 1988.

21. Paris, D., W. Leach, Jr., and E. Joy, "Basic theory of probe-compensated near-field measurements," *IEEE Trans. on Antennas and Propagation*, Vol. 26, No. 3, 373–379, May 1978.
22. Burgos, S., "Contribution to the uncertainty evaluation in the measurement of the main antenna parameters," Ph.D. Dissertation, Technical University of Madrid, 2009.
23. Pivnenko, S., J. E. Pallesen, O. Breinbjerg, M. Sierra Castañer, P. Caballero Almena, C. Martinez Portas, J. L. Besada Sanmartin, J. Romeu, S. Blanch, J. M. Gonzalez-Arbesu, C. Sabatier, A. Calderone, G. Portier, H. Eriksson, and J. Zackrisson, "Comparison of antenna measurement facilities with the DTU-ESA 12 GHz validation standard antenna within the EU antenna centre of excellence," *IEEE Trans. on Antennas and Propagation*, Vol. 57, No. 7, 1863–1878, 2009.
24. Burgos, S., S. Urosa, M. Sierra-Castañer, C. Martinez-Portas, and J. L. Besada, "Uncertainty analysis in antenna measurements," *3rd European Conference on Antennas and Propagation, EuCAP 2009*, 2182–2185, Mar. 23–27, 2009.
25. Newell, A. C., "Error analysis techniques for planar near-field measurements," *IEEE Trans. on Antennas and Propagation*, Vol. 36, No. 6, 754–768, Jun. 1988.
26. Habersack, J., J. Hartmann, J. Lemanczyk, P. de Maagt, and H.-J. Steiner, "Facility trade-off for measurements up to 500 GHz," *Proc. 22nd AMTA*, Philadelphia, USA, Oct. 2000.
27. Alexandridis, A., C. Sabatier, H. Eriksson, J. Zackrisson, L. J. Foged, L. Durand, M. Boettcher, M. Sierra-Castañer, S. Burgos, and S. Pivnenko, "Recommendations and comparative investigation for near-field antenna measurement techniques and procedures," Deliverable A1.2D2, Workpackage WP 1.2-2' Standardization of Antenna Measurement Techniques, Contract FP6-IST 026957, Antenna Centre of Excellence (ACE), Dec. 2007.
28. Gentle, D. G., A. Beardmore, J. Achkar, J. Park, K. MacReynolds, and J. P. M. de Vreede, "Measurement techniques and results of an intercomparison of horn antenna gain in IEC-R 320 at frequencies of 26.5, 33.0 and 40.0 GHz," NPL Report CETM 46, Sep. 2003.
29. Newell, A. C. and G. Hindman, "Techniques for reducing the effect of measurement errors in near-field antenna measurements," *2nd European Conference on Antennas and Propagation, EuCAP 2007*, 1–5, Nov. 2007.